Desalination and Water Treatment
www.deswater.com

doi:10.5004/dwt.2019.23178

139 (2019) 88–94
January

CFD simulation of seawater desalination through a rectangular electrodialysis cell

Alireza Fazlali[a,*], Vahab Ghaleh Khondabi[a], Arash Tayyebi[a], Mostafa Keshavarz Moraveji[b]

[a]*Department of Chemical Engineering, Faculty of Engineering, Arak University, BasijSQ, P.O. Box 38156-88349 Arak, Iran, Tel. +989188614867, email: a-fazlali@araku.ac.ir (A.R. Fazlali), v-ghalehkhondabi@phd.araku.ac.ir (V.G. Khondabi), arash.tayyebi@chmail.ir (A. Tayyebi)*

[b]*Department of Chemical Engineering, Amirkabir University of Technology (Tehran Polytechnic), Hafez Ave, P.O. Box 15875-4413 Tehran, Iran, Tel. +989363098063, email: moraveji@aut.ac.ir (M.K. Moraveji)*

Received 10 January 2018; Accepted 21 September 2018

ABSTRACT

Electrodialysis (ED) is one of the membranous process for seawater desalination, which due to the less energy consuming is a desirable method in comparison with other ones such as thermal methods. In this investigation, computational fluid dynamics (CFD) modeling approach for the simulation of ED unit was studied. Fluid dynamics and ion transfer were simulated using the Navier-Stokes and Nernst-Planck equations, respectively and they were solved via finite element method (FEM). The effects of operating parameters i.e. feed concentration, temperature and voltage on the separation process were evaluated and their best value for obtaining the optimal separation percentage (SP) were determined. The concentration of 10000, 20000 and 40000 ppm, the temperature of 25, 40 and 55°C, and the voltage of 5, 7, 9 V were used to determine impressive parameters in simulation. The results showed that the highest efficiency were obtained at high temperatures and voltage and lowest feed concentration, which was good agreement with observed ones. Moreover, the average deviation from experimental data was less than 2% for optimum condition.

Keywords: CFD model; Comsol; ED; FEM; Seawater desalination

1. Introduction

Seawater is not appropriate for agricultural and nutrition purposes due to the fact that it contains huge amount of salts. Hence, desalination is an increasingly common solution to supply fresh water in many regions of the world, especially the areas threatened by water scarcity [1]. In the past few years, several wastewater treatment processes have been proposed to be effective for water reuse, with special emphasis on waste minimization and hazardous waste treatment. However, decreasing the energy requirements and infrastructure costs of existing desalination technologies still remain a challenge [2]. In general, desalination technologies can be categorized into two different mechanism separations, i.e. thermal and membrane-based desalination [3]. Nowadays, membrane technologies are receiving more and more attention due to their reliable contaminant removal without production of any harmful by-products, especially in water and wastewater treatment [4,5].

The ED process uses direct current power to remove salts and other ionized species with alternating anion (AM) and cation (CM) exchange membranes [6]. The use of ED is particularly significant because it approaches membrane technology as an advanced environmental technology that enables the development of clean treatment sequences for the recovery of water in industrial processes [7].

P. Moon et al. [8] analyzed three models formulations for batch and continuous ED in a single salt (KCl). They showed that the ionic surface concentration in the dilute compartment is affected by flow rate and current density, they also observed that the concentration changes and ionic flux along the x-axis are greater than along the y-axis.

*Corresponding author.

L. Firdaous et al. [9] developed a mathematical model to describe the mass transport of ED of NaCl solution based on the Stefan-Maxwell equations. They estimated some diffusivity and the ion distribution inside membranes.

Casas et al. [10] used Nernst-Planck equations to predict the performance of ED pilot plant for concentrate NaCl in order to be reused in the chlor-alkali industry. Their model accurately predicted the optimum conditions to reach the maximum NaCl concentration.

Fadaei et al. [11] studied the effect of concentration polarization phenomenon on the ion separation through the nanoporous membranes. They predicted the local concentration of ions, flux of permeate, and rejection of ions using a combination of two transport models.

Tamburini et al. [12] carried out CFD simulation in order to predict the fluid flow field inside a reverse electrodialysis (RED) channel. They investigated the relation between the pressure drops and the fluid flow rate for some different channel configurations.

Sousa et al. [13] used CFD techniques to study the hydrodynamics of feed channels of a desalination membrane filled with spacers in zigzag arrangements and transverse in relation to the flow. Their results show a very good agreement with the experimental data.

Zourmand et al. [14] predicated of ion transport through ED cells by a combination of three-layer model and convection-diffusion model. They solved the model's equation by CFD in three sub-domains of dilute, concentrate cells and membranes.

Gurreri et al. [15] developed a multi-physical model of RED units using the Navier–Stokes, Nernst–Planck and Donnan equations. They investigated the effect of the various operating parameters and different membrane/channel geometrical configurations.

Moya [16] studied the behavior of a bilayer ion-exchange membrane in a RED stack. He obtained the thickness of the diffusion boundary layer, using the numerical solution on the basis of the Nernst-Planck-Donnan equations under electrical neutrality conditions in the Teorell-Meyer-Sievers model.

In this study, experimental data of seawater desalination using ED [17] were numerically simulated using CFD techniques and the effect of operating condition i.e. feed concentration, temperature and voltage on performance of an ED cell was investigated.

2. CFD modeling

A hydrodynamic theory of desalination by ED consists of two major areas developed for a laminar flow between parallel membranes. One of these problems is associated with the membranes and the other is from a hydrodynamic point of view, which depends on the detailed flow phenomena in the system.

2.1. Basic conservation equations

The governing equations of transport phenomena consist of momentum and mass transfer applied simultaneously for numerical solution of problem under the assumptions of steady state operation, laminar flow and incompressible fluid.

- Momentum equation:

$$\nabla \cdot u = 0 \tag{1}$$

$$\rho \frac{\partial u}{\partial t} + \rho u \nabla \cdot u = -\nabla p + \mu \nabla^2 u \tag{2}$$

Eqs. (1) and (2) are the continuity and Navier-Stokes equations used to obtain the velocity field in channels, where ρ (kg/m^3), u (m/s), t (s), p (Pa) and μ(Pa.s) are the density of the fluid, velocity vector, time, pressure and dynamic viscosity, respectively.

- Energy equation:

$$\frac{\partial}{\partial t}(\rho h) + \nabla \cdot \left(\rho u C_p T\right) = \nabla \cdot \left(k \nabla T\right) \tag{3}$$

where u (m/s), t (s), T (K), ρ (kg/m^3), C_p (J/kg·K), k (W/m·K) and h (W/m^2·K) are velocity vector, time, temperature, density of the fluid, specific heat, thermal conductivity and heat transfer coefficient, respectively.

- Mass equation:

Usually, mass transfer equations are combined with other equations describing hydrodynamic conditions and solved simultaneously to obtain the concentration distribution of the solute. Mass transport of ionic species is described in the Nernst-Planck approach by the following equation (diffusion + migration + convection):

$$N_i = -D_i \nabla c_i - z_i m_i F c_i \nabla \varnothing + u c_i \tag{4}$$

where N_i (mol/m^2·s) is the total flux of species i. The first term is the diffusion flux and D_i (m^2/s) and c_i (mol/m^3) are the diffusion coefficient and the concentration of species i, respectively. The second term shows the migration flux, which consists of the species charge number z_i, the species mobility m_i (s·mol/kg), Faraday's constant F (C/mol) and the electrical potential φ (v). In the convection term, u denotes the fluid velocity vector (m/s).

It is assumed that the salt in the solution is dissociated perfectly. A consequence of this assumption is that the diffusion equations for the ions are simplified in which the concentration is replaced with activity, and the diffusion coefficient and mobility are related by Einstein's relation. Finally, there is one positive and one negative charged species and these do not enter into any reaction in the bulk of the fluid [18]. Table 1 shows the diffusion coefficient of sodium and chlorine in water at 25, 40 and 55°C.

Table 1
Diffusion coefficient of sodium and chlorine at variation temperature

Temperature (°C)	D_{Na} (10^{-9} m^2·s^{-1})	D_{Cl} (10^{-9} m^2·s^{-1})
25	1.334	2.032
40	1.909	2.908
55	2.580	3.930

2.2. Model geometry and boundary conditions

Fig. 1 shows the schematic view of the simulation geometry and mesh. This schematic consists of two ion selective membranes: left hand side membrane is assumed to be permeable to cations only, and the other is permeable to anions only. The middle domain is a free flowing electrolyte, where salt is to be removed (dilute compartment). The rightmost and leftmost domains are free flowing electrolyte domains, where the ion concentration will increase during the cell operation (concentrate compartment). In the free electrolyte domains, the flow enters at the bottom inlets and exits at the top outlets at temperatures of 25, 40, and 55°C, an average flow rate is 0.07 ml/s. The cell is fed with a seawater electrolyte consisting of 10000, 20000, and 40000 ppm NaCl, and operated at unit cell voltages of 5,7 and 9 V. The thickness of dilution cell (center), each concentrate cell (left and right) and ion exchange membranes are 4, 3 and 3 mm, respectively. As well as effective area of each membrane is 60 × 65 mm^2.

The model equations including continuity, momentum and transport equations related to the channels and membrane with appropriate boundary conditions are numerically solved by finite element method (FEM) approach and using COMSOL 5.2 a Multi-physics software.

In order to check the mesh independency, different mesh sizes are tried. By increasing the number of nodes more than 25920, the concentration changes no more. This indicates that a solution value that is independent of the mesh resolution is achieved. So for further analysis a mesh with 25920 nodes is used to give results due to acceptable accuracy and less computational time. Fig. 1 shows a segment of the mesh which is used to determine the ion transport behavior through the channels and membranes.

3. Results and discussion

In this study, the effect of different experimental conditions on SP were evaluated and a comparison was carried out between the simulation results and the experimental results. The quality characteristic was SP which was calculated as follows:

$$SP = \frac{C_0 - C}{C_0} 100 \quad (5)$$

where C_0 and C are feed and dilute concentrations, respectively.

3.1. Concentration distribution in channels

Fig. 2 illustrates the concentration distribution in compartments at 55°C, 10000 ppm and 5 V. It is observed that the concentration increases in the concentrate compartment, and decreases in the dilute compartment. A boundary layer with high concentration gradient forms close to the membrane surfaces (polarization layer).

3.1.1. Concentration distribution in fixed voltage and feed concentration

Fig. 3 illustrates the concentration distribution at three different temperatures (25, 40 and 55°C) and constant feed concentration and voltage (10000 ppm and 9 V). The concentration gradients increase with the increase of temperature, and on the basis of Eq. (4), SP increases.

Fig. 4 indicates the values of separation obtained from the simulation compared with experimental data. As it can be seen in the figure, temperature is directly proportional to SP, the electrical conductive coefficient has been raised by increasing temperature in addition of decreasing electrical resistance which resulted in the enhancement of ionic motion speed. As well as the increase in temperature decreases the viscosity of the electrolyte solution and increase diffusion coefficient of ions which are effective on the separation percent.

3.1.2. Concentration distribution in fixed temperature and feed concentration

Fig. 5 indicates the concentration distribution in 55°C and 10000 ppm of feed concentration in the variable voltages

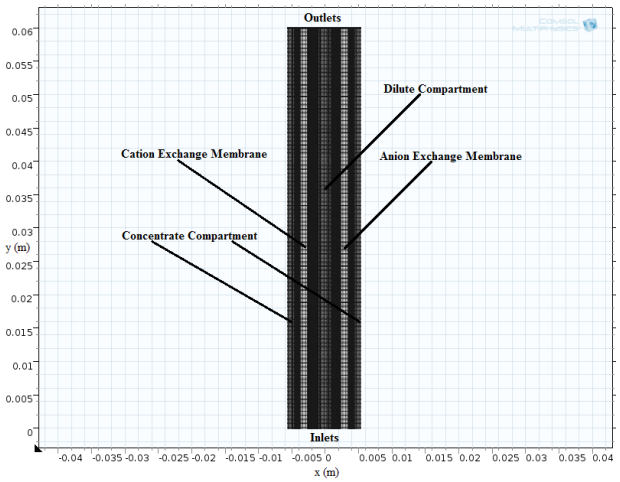

Fig. 1. Schematic view of the simulation geometry and mesh.

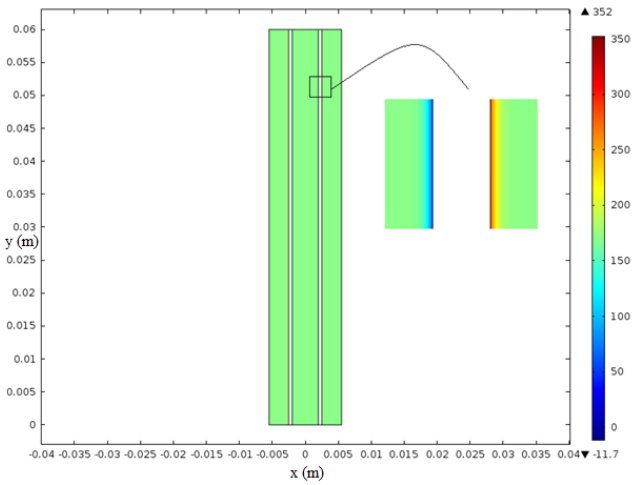

Fig. 2. Concentration profile in channels (55°C, 10000 ppm and 5V).

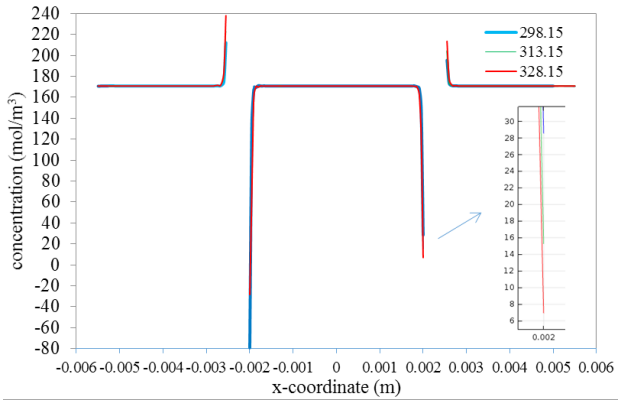

Fig. 3. Ion concentration at half of the cell height for different temperatures (10000 ppm and 9 V).

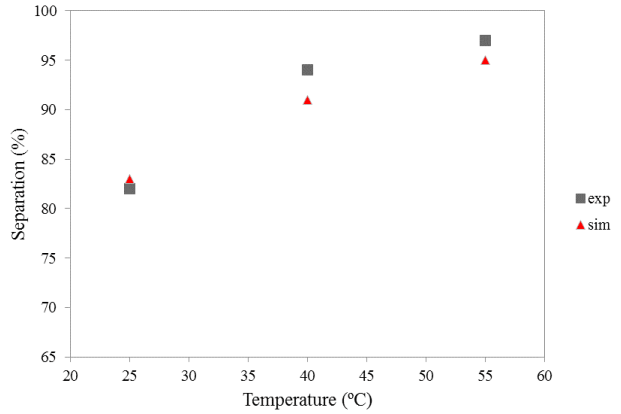

Fig. 4. Comparison of separation percent by this simulation and experimental values (10000 ppm and 9 V).

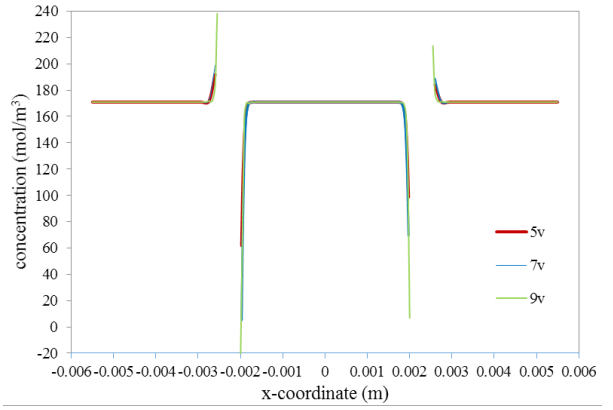

Fig. 5. Ion concentration at half of the cell height for different voltage (10000 ppm and 55°C).

(5, 7 and 9 V).The concentration gradients increase with the increase of voltage, which results in an increase in SP.

The comparison between the results of simulation and experimental data have been shown in Fig. 6. As expected, by increasing the voltages, that is the main factor of driving force for ED process, the SP increases, also this figure indicated that the accuracy of simulation is very good.

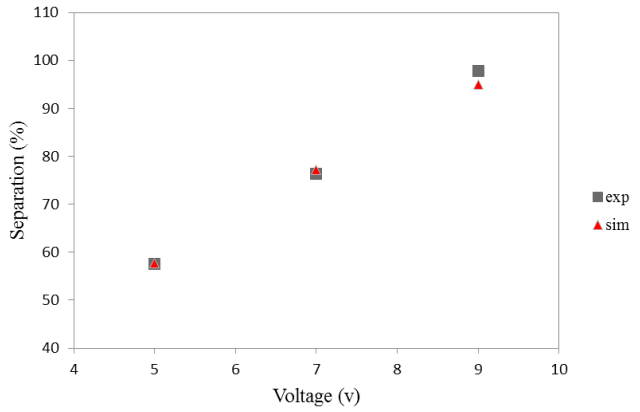

Fig. 6. Comparison of separation percent by this simulation and experimental values (10000 ppm and 55°C).

3.1.3. Concentration distribution in fixed temperature and voltage

Fig. 7 demonstrates the concentration distribution of compartments at a constant temperature (55°C) and constant voltage drop (9 V) in different feed concentrations (10000, 20000 and 40000 ppm).The concentration gradients decrease with the increase of feed concentration that will reduce the SP.

Fig. 8 illustrates the values of SP by simulation and its comparison with the experimental data. As we know, in a constant driving force at lower feed concentration, in spite of the fact that solution conductivity decreases, SP increases. At higher feed concentration, SP decreases due to concentration polarization phenomenon at high concentrations and limited ion exchange capacity of the membrane.

3.2. Effect of voltage on separation percent at different feed concentration

Figs. 9, 10 and 11 illustrate the distribution of concentration in compartments at constant temperature (40°C) different voltages and feed concentrations. As it can be seen from Table 2, while increasing voltage, the electrical resistance of the feed solution decreases and subsequently ED separation performance increases. Furthermore, in the best operating conditions (40°C, 10000 ppm and 9 V), simulation and experimental separation percent were 91 and 93%, respectively that indicates, the simulation results are in good agreement with experimental results (deviation of 2.2%).

3.3. Effect of temperature on separation percent at different voltages

Figs. 12 and 13 illustrate the concentration distribution at constant feed concentration (20000 ppm) and different temperatures and voltages. As it have been shown in Table 3, while increasing temperature, the electrical conductive coefficient increases that resulted the raise of SP. Also, in the best operating condition (20000 ppm, 55°C and 7 V), separation percent of simulation and experimental were 66 and 66.7% respectively,which shows that the model had a good prediction of experimental results (deviation of 1.06%).

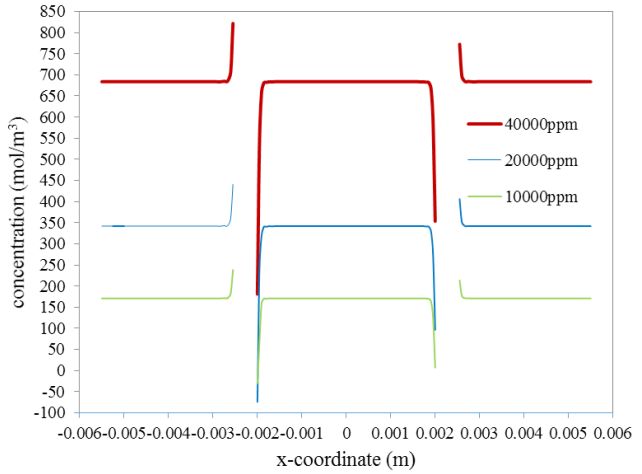

Fig. 7. Ion concentration at half of the cell height for different feed concentrations (55°C and 9 V).

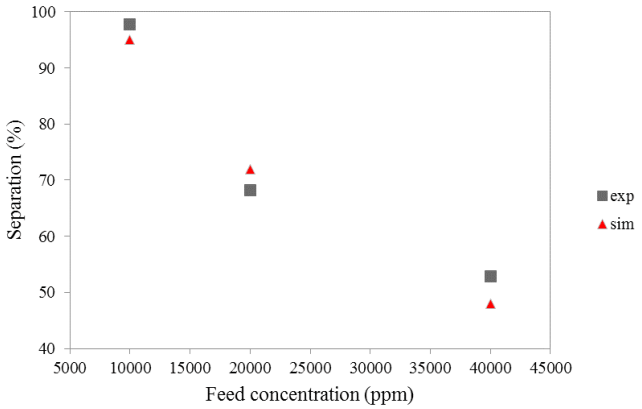

Fig. 8. Comparison of separation percent by this simulation and experimental values (9 V and 55°C).

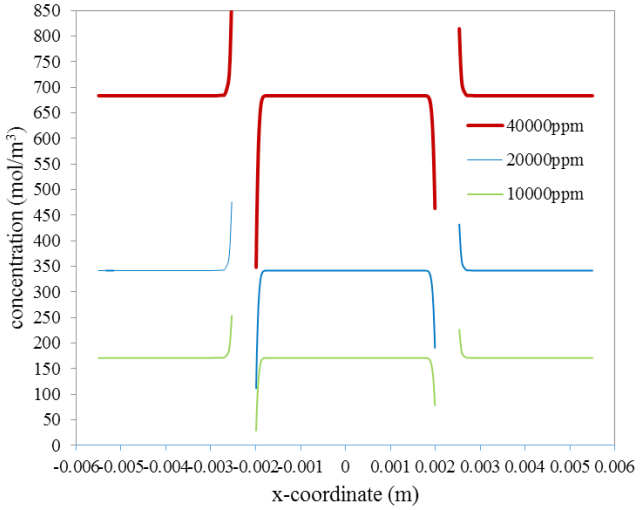

Fig. 9. Ion concentration at half of the cell height for different feed concentrations (40°C and 5 V).

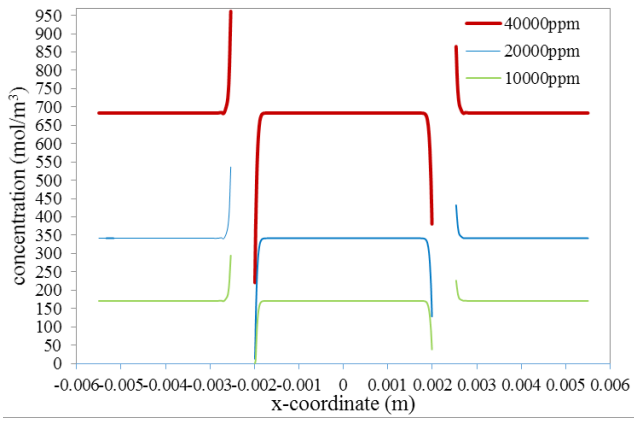

Fig. 10. Ion concentration at half of the cell height for different feed concentrations (40°C and 7 V).

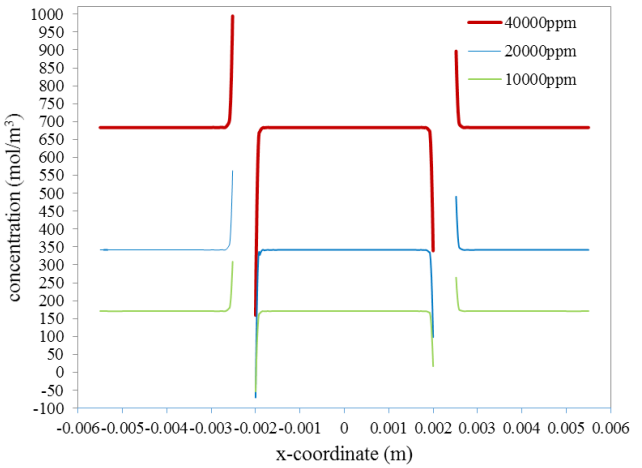

Fig. 11. Ion concentration at half of the cell height for different feed concentrations (40°C and 9 V).

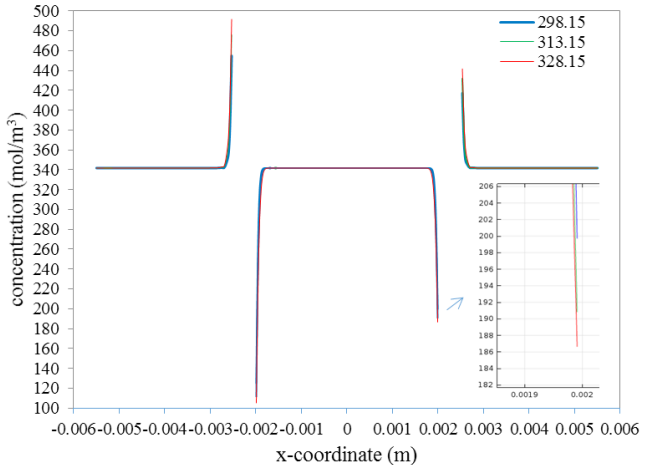

Fig. 12. Ion concentration at half of the cell height for different temperatures (20000 ppm and 5 V).

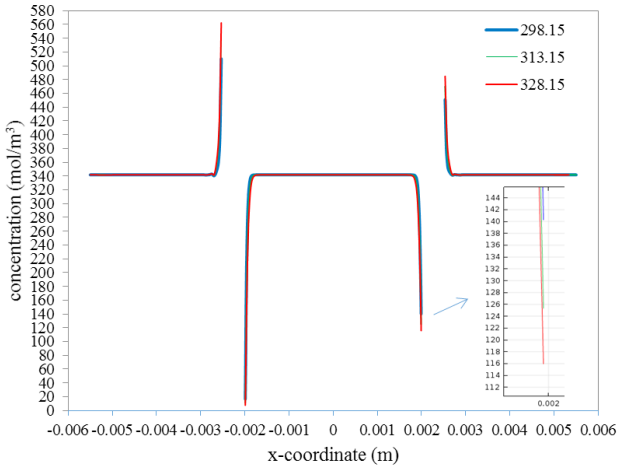

Fig. 13. Ion concentration at half of the cell height for different temperatures (20000 ppm and 7 V).

Table 2
Comparison of separation percent by this simulation and experimental values for 40°C and different feed concentration and voltage

Operating parameters			SP (%)	
T (°C)	C (ppm)	V (v)	Simulation	Experimental
40	10000	5	54	50
40	10000	7	77	73
40	10000	9	91	93
40	20000	5	44	47
40	20000	7	62	64
40	20000	9	71	70
40	40000	5	32	42
40	40000	7	45	47
40	40000	9	50	51

Table 3
Comparison of separation percent by this simulation and experimental values for 20000 ppm and different temperature and voltage

Operating parameters			SP (%)	
C (ppm)	T (°C)	V (v)	Simulation	Experimental
20000	25	5	41	41.8
20000	25	7	59	59.0
20000	40	5	44	47.0
20000	40	7	62	64.0
20000	55	5	45	48.0
20000	55	7	66	66.7

4. Conclusions

This work presented a numerical study on seawater desalination using ED process. The aim of this study was determining the most accurate condition to examine the effect of variation of feed concentration, temperatures and voltages on the individual ions SP and efficiency. By increasing the voltage in constant temperature and feed concentration, SP of ED increased. At constant temperature and voltage, decrease in the feed concentration led to the increase of SP. Increasing the temperature enhances the rate of separation at constant voltage and feed concentration. As a result, higher temperature and voltage and fewer feed concentration were recommended to modify performance of ED cell.

The results of the modeling were compared with the experimental values, which indicated that the simulation has acceptable accuracy. In addition, the performed simulation to reduce the time and cost for testing ED cell membranes, also be able to specify the optimal values of effectual parameters to achieve maximum SP which are important in separation efficiency and increasing membrane lifetime.

Symbols

C — Concentration (mol·m^{-3})
C_p — Specific heat (J·kg^{-1}·K^{-1})
D — Diffusion coefficient (m^2·s^{-1})
F — Faraday's constant (C·mol^{-1})
h — Heat transfer coefficient (W·m^{-2}·K^{-1}))
k — Thermal conductivity (W·m^{-1}·K^{-1})
m — Mobility (s·mol·kg^{-1})
N — Flux (mol·m^{-2}·s)
p — Pressure (Pa)
t — Time (s)
T — Temperature (°C)
u — Velocity vector (m·s^{-1})
V — Voltage (V)
x — Longitudinal rectangular coordinate (m)
y — Transverse rectangular coordinate (m)
Z — Charge number

Greek

μ — Dynamic viscosity (Pa·s)
ρ — Density (kg·m^{-3})
∅ — Electrical potential (v)

Subscripts

i Species i (Na$^+$, Cl$^-$, fixed charges)

Abbreviations

AM — Anion membrane
CFD — Computational fluid dynamics
CM — Cation membrane
ED — Electrodialysis
FEM — Finite element method
RED — Reverse electrodialysis
SP — Separation percent

References

[1] B. Penate, L. Garcia-Rodriguez, Current trends and future prospects in the design of seawater reverse osmosis desalination technology, Desalination, 284 (2012) 1–8.

[2] T. Humplik, J. Lee, S.C.O. Hern, B.A. Fellman, M.A. Baig, S.F Hassan, M.A. Atieh, F. Rahman, T. Laoui, R. Karnik, E.N. Wang, Nanostructured materials for water desalination, Nanotechnology, 22 (2011) 1–19.
[3] A.M. Bernardes, M.A.S. Rodrigues, J.Z. Ferreira, Electrodialysis and Water Reuse: Novel Approaches, Springer-Verlag Berlin and Heidelberg GmbH & Co. KG, 2014 Ed.
[4] N. Misdan, W.J. Lau, A.F. Ismail, Seawater Reverse Osmosis (SWRO) desalination by thin-film compositemembrane-Current development, challenges and future prospects, Desalination, 287 (2012) 228–237.
[5] K. Venugopal, S. Dharmalingam, Desalination efficiency of a novel bipolar membrane basedon functionalized polysulfone, Desalination, 296 (2012) 37–45.
[6] J.M. Ortiz, J.A. Sotoca, E. Exposito, F. Gallud, V. Garcia-Garcia, V. Montiel, A. Aldaz, Brackish water desalination by electrodialysis: batch recirculation operation modeling, J. Membr. Sci., 252 (2005) 65–75.
[7] A. Basile, S.P. Nunes, Advanced Membrane Science and Technology for Sustainable Energy and Environmental Applications, Woodhead Publishing Series in Energy, 24th August 2011.
[8] P. Moon, G. Sandi, D. Stevens, R. Kizilel, Computational modeling of ionic transportin continuous and batch electrodialysis, Sep. Sci. Technol., 39 (2004) 2531–2555.
[9] L. Firdaous, T. Saheb, J.-P. Schlumpf, J.-P. Maleriat, P. Bourseau, P. Jaouen, A mathematical model of multicomponent mass transfer in electrodialysis, Scandinavian Conference on Simulationand Modeling, Trondheim, Norway, October 13–14, 2005.
[10] S. Casas, N. Bonet, C. Aladjem, J.L. Cortina, E. Larrotcha, L.V. Cremades, Modelling sodium chloride concentration from seawater reverse osmosis brine by electrodialysis: preliminary results, Solvent. Extr. Ion Exc., 29 (2011) 488–508.
[11] F. Fadaei, S. Shirazian, S.N. Ashrafizadeh, Mass transfer modeling of ion transport through nanoporous media, Desalination, 281 (2011) 325–333.
[12] A. Tamburini, G. La Barbera, A. Cipollina, M. Ciofalo, G. Micale, CFD simulation of channels for direct and reverse electrodialysis, Desal. Water Treat., 48 (2012) 370–389.
[13] P. Sousa, A. Soares, E. Monteiro, A. Rouboa, A CFD study of the hydrodynamics in a desalination membrane filled with spacers, Desalination, 349 (2014) 22–30.
[14] Z. Zourmand, F. Faridirad, N. Kasiri, T. Mohammadi, Mass transfer modeling of desalination through an electrodialysis cell, Desalination, 359 (2015) 41–51.
[15] L. Gurreri, G. Battaglia, A. Tamburini, A. Cipollina, G. Micale, M. Ciofalo, Multi-physical modelling of reverse electrodialysis, Desalination, 423 (2017) 52–64.
[16] A.A. Moya, Numerical simulation of ionic transport processesthrough bilayer ion-exchange membranes in reverse electrodialysis stacks, J. Membr. Sci., 524 (2017) 400–408.
[17] M. Sadrzadeh T. Mohammadi, Sea water desalination using electrodialysis, Desalination, 221 (2008) 440–447.
[18] E. Samson, J. Marchand, K.A. Snyder, Calculation of ionic diffusion coefficients on the basis of migration test results, Mater. Struct., 36 (2003) 156–165.